Nanotechnology and Nano-Interface Controlled Electronic Devices
Editors: M. Iwamoto, K. Kaneto and S. Mashiko

CHAPTER 5

Control of molecular selective-assembling on metal surface

Takashi Yokoyama [a], Toshiya Kamikado [b], Shiyoshi Yokoyama [b], Yoshishige Okuno [b], and Shinro Mashiko [b]

[a] *National Institute for Materials Science, 2268-1 Shimo-shidami, Moriyama-ku, Nagoya 463-0003, Japan*
[b] *Communications Research Laboratory, 588-1 Iwaoka, Nishi-ku, Kobe 651-2401, Japan*

1. Introduction

The realization of molecular nanodevices with advanced functions requires the development of new approaches to construct desired molecular nanostructures [1,2]. Supramolecular approach starting from molecular building blocks can lead to controlled structures [3], which is achieved by selective and directional intermolecular interactions. When non-covalent intermolecular interactions such as hydrogen bonding are introduced into functional molecules, the selective intermolecular interaction results in the controlled formation of molecular nanostructures, which have yielded exclusively crystals or dissolved structures [3]. To adapt the functional supramolecular structures to nanodevices, it should be necessary for the supramolecular structures to be supported on suitable substrates and at suitable positions.

On substrate surfaces, atomic-scale investigation of adsorbed molecules has been enabled by using scanning probe microscopy, particularly scanning tunneling microscopy (STM) [4]. In particular, recent advance of high-resolution STM imaging allows one to directly determine their arrangement, configuration, and conformation of individual largish molecules on surfaces [5–9]. Based on the submolecular-resolution STM studies

and on theoretical calculations, several groups have been reported specific interactions of adsorbed molecules on metal surfaces [10–12], revealing self-assembled aggregation on surfaces.

Whereas these surface-supported supramolecular structures have been directly observed using STM, the further control of their size and shape on surfaces should become a next step for realizing molecular nanodevices. In this work, we demonstrate selective assembly of supramolecular aggregates with controlled size and shape on a gold surface by modifying substituent structures.

2. H_2-TBPP and Au(111) as basic molecule and substrate

The basic molecule used in this study is 5,10,15,20-tetrakis-(3,5-di-tertiarybutylphenyl) porphyrin (H_2-TBPP), which has a free-base porphyrin core and four di-tertiarybutylphenyl (tBP) substituents, as shown in Fig. 1(a). An ideal shape of H_2-TBPP exhibits a planar macrocyclic conformation of the central porphyrin through 60°–90° rotation of the phenyl rings with respect to the phenyl mean plane, as shown in Fig. 1(b), obtained from semi-empirical molecular orbital calculations. By the bulky tBP substituents, the aromatic π system of the central porphyrin should be sterically decoupled to the substrate surface even after adsorption, fulfilling the requirements for the molecular nanoelectronic or optoelectronic devices [5,6,13]. To understand the conformation and arrangement of the H_2-TBPP molecules, all experiments were performed in an ultrahigh-vacuum (UHV) chamber with a low-temperature STM. A Au(111) surface was used as a substrate because of its inertness and its properties of reconstruction. The atomically clean surface of Au(111), which was formed by deposition of Au on mica in UHV, was prepared by repeated cycles of Ar^+ sputtering and annealing at 700 K. Fig. 2 shows an STM image of the reconstructed Au(111) at 63 K. The reconstruction of the Au(111) surface results from alternating face centered cubic (fcc) and hexagonal close packed (hcp) stacking of the surface atoms with respect to the bulk lattice, and long-range "herringbone" patterns are formed by periodic rotations of the uniaxial domains [14,15]. In addition, each elbow of this pattern contains a dislocation of the surface lattice, and the preferential nucleation of adsorbates at the elbows has been observed in various systems [12,16].

3. Nonplanar conformation and orientational ordering of H_2-TBPP on Au(111)

The H_2-TBPP molecules were deposited onto the Au(111) surface at room temperature by sublimation from a Knudsen cell in UHV. The sample was then subsequently transferred to the cooled STM stage for direct observation. Fig. 3(a) shows an STM image of the Au(111) surface at 63 K after a small amount of the H_2-TBPP deposition. In this image, most of the molecules are located at the elbows of the surface reconstructed patterns, revealing regular arrays of isolated single molecules. In this system, it should be noted that the selective molecular positioning allows direct imaging of isolated single molecules without intermolecular interactions. Fig. 3(b) shows the high-resolution STM

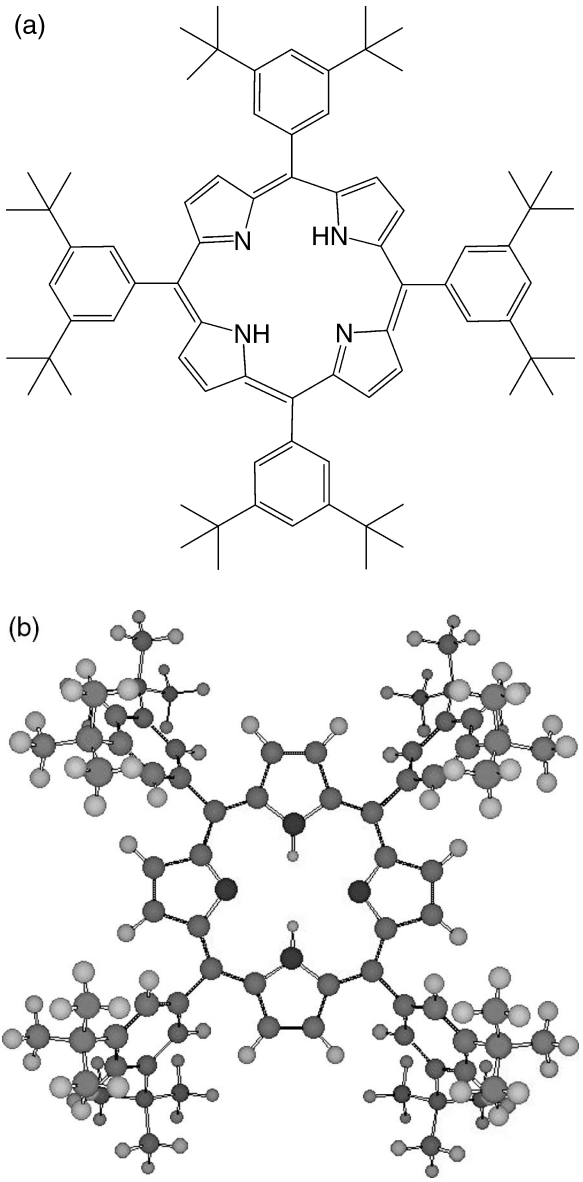

Fig. 1: (a) A structure of H_2-TBPP, which includes the central free-base porphyrin and four tBP substituents. (b) Calculated conformation of H_2-TBPP, obtained from the semi-empirical molecular orbital method. The about 65° rotations of phenyl rings results from steric hindrance between the porphyrin and phenyl rings.

image of a single H_2-TBPP molecule on the Au(111) surface at 63 K, which exhibits four paired lobes surrounding two oblong protrusions. From the molecular dimension, we assign each lobe as one of the tertiary-butyl substituents, and the appearance of

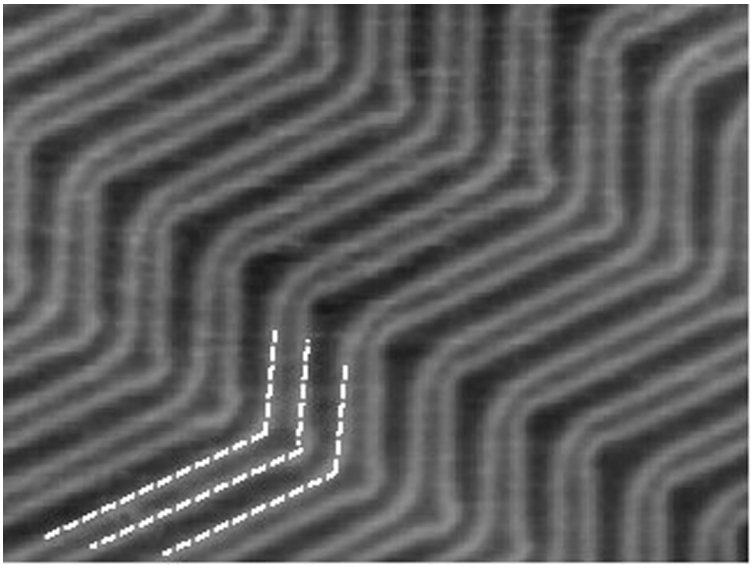

Fig. 2: STM image (70 nm × 53 nm) at 63 K of an Au(111) surface, in which bright stripes are associated with domain walls between fcc and hcp stackings, as indicated by dashed lines, and the herringbone patterns are formed by periodic rotations of the uniaxial domains.

the paired lobes suggests that the phenyl rings are oriented close to the porphyrin macrocyclic plane, different from the ideal conformation of H_2-TBPP shown in Fig. 1(b). In this high-resolution image, each of the paired lobes consists of brighter and darker ones, and the lateral distance is estimated to be about 4.5 Å. By comparing the STM results with the molecular model, we have derived the dihedral angle between the porphyrin and phenyl rings to be about 20°, where the four phenyl rings are alternately rotated with respect to the porphyrin mean plane. The rotations of the phenyl–porphyrin bonds have been reported for adsorbed Cu-TBPP molecules on several metal surfaces, which depend on the substrate structures [6,9]. These results indicate that the rotational flexibility of the phenyl–porphyrin bonds allows the tertiary-butyl substituents to fit into the surface geometry, leading to the conformational changes.

In the STM image of Fig. 3(b), the most distinguishing feature is that the internal structure of the central porphyrin has been resolved in the STM image, which is composed of the two oblong protrusions. We observed that the STM images were independent of the bias polarity, suggesting that the atomic structure was mainly contributed in the STM image, compared with the electronic structure. Thus, the oblong protrusions should be associated with the nonplanar deformation of the central porphyrin, induced by the rotations of the phenyl-based substituents. To confirm the nonplanar macrocyclic conformation, we performed the semi-empirical molecular orbital calculations with the AM1 hamiltonian [18]. Fig. 3(c) shows the calculated conformation of H_2-TBPP with fixed 20° rotations of the four phenyl rings with respect to the central porphyrin. The relaxed structure shows that the 20° alternate rotations

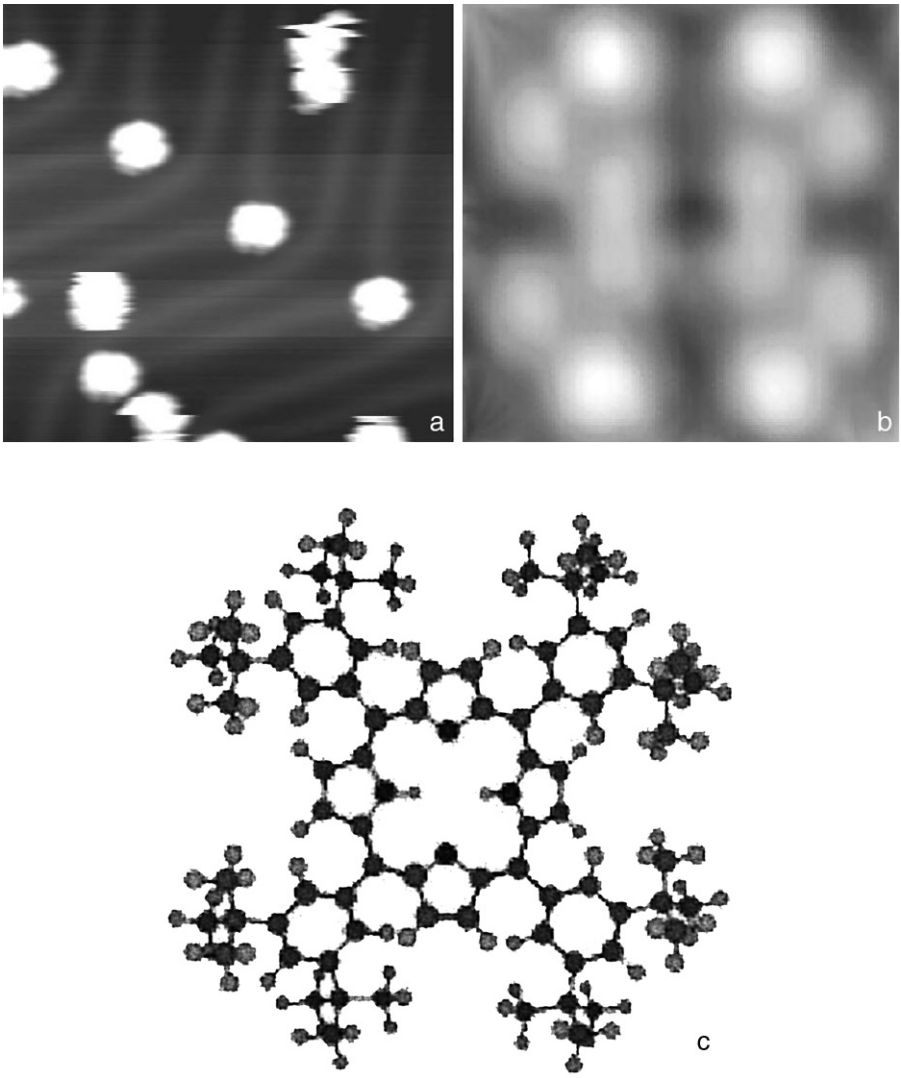

Fig. 3: (a) STM image (20 nm × 20 nm) of the Au(111) surface at 63 K after a small amount of the H_2-TBPP deposition. A regular array of single molecules results from preferential adsorption at the elbows of the herringbone patterns. (b) High-resolution STM image (2.1 nm × 2.1 nm) at 63 K of a single H_2-TBPP molecule, which is composed of four paired lobes surrounding two oblong protrusions. (c) Top view of calculated macrocyclic conformation of the H_2-TBPP molecule with 20° alternate rotations of the phenyl rings, obtained using semi-empirical molecular orbital calculations. A saddle-shaped nonplanar deformation of the central porphyrin is induced by the steric interactions with the rotated phenyl rings.

of the phenyl rings induce nonplanar deformation of the porphyrin macrocycle, while the ground state conformation is formed through about 65° rotations as shown in Fig. 1(b). In this nonplanar conformation, the saddle-shaped deformation of the central

porphyrin is characterized by alternately tilting of pyrrole rings above and below the mean plane, which should be induced by steric hindrance with the rotated phenyl rings. The maximum deviation of the porphyrin macrocycle from the mean plane is estimated to be about 0.95 Å, which is roughly consistent with the STM corrugations of 0.6 Å. In the high-resolution STM image of Fig. 3(b), the two oblong protrusions should be associated with the tilt-up pyrrole rings of the nonplanar porphyrin macrocycle, whereas the tilt-down pyrrole rings weakly appear as bridges between two oblong protrusions. In addition, we have obtained similar STM images for Cu-TBPP molecules on the Au(111) surface at 63 K. Due to the symmetric structure of the central Cu-porphyrin, this result should exclude a possibility that the two oblong protrusions are related to the electronic asymmetry of the central H_2-porphyrin.

With increasing coverage of H_2-TBPP onto the Au(111) surface, two-dimensional islands are formed through self-assembled aggregation. As shown in Fig. 4(a), we have observed larger islands even without thermal annealing, suggesting a low diffusion barrier of the adsorbed molecules on the surface. In the islands, the nonplanar macrocyclic conformation remains, and the molecules exhibit a close-packed arrangement on the surface [Fig.4(b)]. A detailed analysis of the STM images indicates that the molecular arrangement exhibits an $11 \times 5\sqrt{3}$ superstructure, commensurate with the underlying substrate lattice of Au(111). Fig. 4(c) shows the model of the H_2-TBPP island formed on the Au(111)-1×1 structure, where intermolecular interactions should be governed by the van der Waals force between the tBP substituents.

Due to the saddle-shaped deformation of the central porphyrin with mirror (C_{2v}) symmetry, the molecular orientations can be determined from directions of a dark line (symmetric axis) in the STM images. As shown in Fig. 5(a) and (c), two different orientations of the nonplanar porphyrins are randomly distributed within the island. We find that an orientational ordering is obtained via a thermal activation process. Fig. 5(b) shows the STM image of the supramolecular island after short thermal annealing (for 1 min at about 470 K). Inside the island, the orientations of neighboring molecules are the same in the $[1\,1\,\overline{2}]$ direction and rotated by 90° in the $[\overline{2}\,1\,1]$ direction, as illustrated in Fig. 5(d). It should be noted that the orientational ordering is accompanied without a change of the molecular arrangement, and such the orientations have been observed over the surface. Because it appears that the degree of the orientational ordering depends on the annealing temperature and time, the transformation should be related to rapid molecular diffusion on the surface, promoting breaking and rearrangement of the molecular islands. This kinetic process might allow the molecular islands to be rearranged in a stable manner.

The orientational ordering should be associated with steric intermolecular interactions between the tBP substituents. Because of the 20° rotations of the phenyl rings, two possible steric interactions are expected between tBP substituents; cross- and parallel-type interactions of the tBP substituents between neighboring molecules in both the $[1\,\overline{1}\,0]$ and the $[1\,1\,\overline{2}]$ direction. The ordered orientations indicate that the cross-type interaction (up–down connections of each tertiary-butyl substituent) should be more stable than the parallel-type one (up–up and down–down connections), although the energy difference might be extremely small.

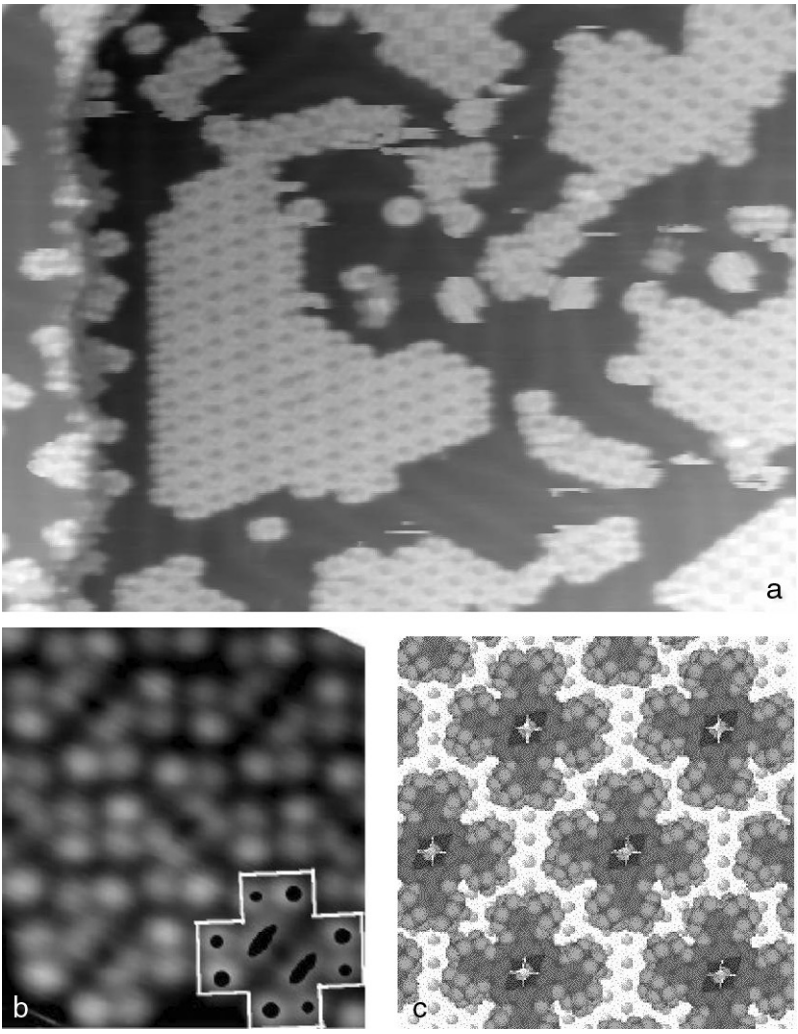

Fig. 4: (a) STM image (65 nm × 50 nm) at 63 K of a H_2-TBPP island formed on the Au(111) surface. (b) and (c) High-resolution STM image (5.3 nm × 5.3 nm) and its model of the H_2-TBPP island, exhibiting an $11 \times 5\sqrt{3}$ superstructure.

4. Selective aggregation of cyanophenyl-substituted porphyrins on Au(111)

The orientational ordering of H_2-TBPP should be due to the weak steric intermolecular interactions between tBP groups. This result indicates that the molecular assembly formed on a surface can be controlled by changing substituents. In supramolecular chemistry, a large number of different selective and directional intermolecular interactions has been developed to control molecular aggregation, although it has been focused mainly on dissolved structures [3]. In this work, we have used a cyanophenyl substituent

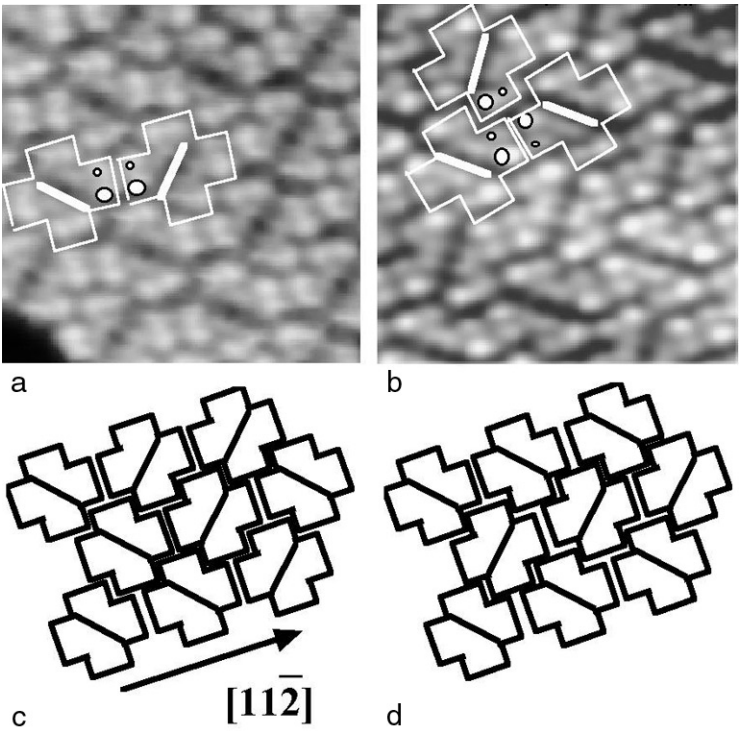

Fig. 5: STM images (9.5 nm × 9.5 nm) of the H_2-TBPP island before (a) and after (b) thermal annealing at about 470 K for 1 min. (c) and (d) Schematic illustrations of the molecular arrangement and orientations within the island [17].

to control the molecular aggregation [19,20], because it has a simple and symmetric structure as well as an asymmetric charge distribution at the cyano group that should introduce dipole–dipole interactions between neighboring cyanophenyl substituents. An illustration of this interaction is given in Fig. 6, which shows the optimized arrangement of a cyanobenzen dimer and trimer obtained in ab initio molecular orbital calculations at the MP2/6-31G* level [20,21]. In the dimer, the cyano groups have an antiparallel configuration, whereas the trimer structure results from a cyclic arrangement of the cyano groups. The length of the CH…NC contacts is about 2.39 Å and 2.65 Å for the dimer and trimer, respectively, and thus shorter than the van der Waals distance of about 2.7 Å. The interaction energies are estimated to be −7.12 kcal/mol and −12.40 kcal/mol for the dimer and trimer structures, respectively, and thus comparable to the energy of hydrogen-bonding interactions. The relative orientation of molecules in these aggregates is therefore likely to be influenced by long-range dipole–dipole interaction, with hydrogen-bonding interactions further stabilizing the structure.

To introduce the characteristic interaction of the cyano substituents, we have synthesized 5-(4-cyanophenyl)-10,15,20-tris(3,5-di-tertiarybutylphenyl) porphyrin (CTBPP), where a tBP group of H_2-TBPP was replaced with a cyanophenyl substituent, as shown in Fig. 7(a). At low coverage, most CTBPP molecules assembled into triangular clusters

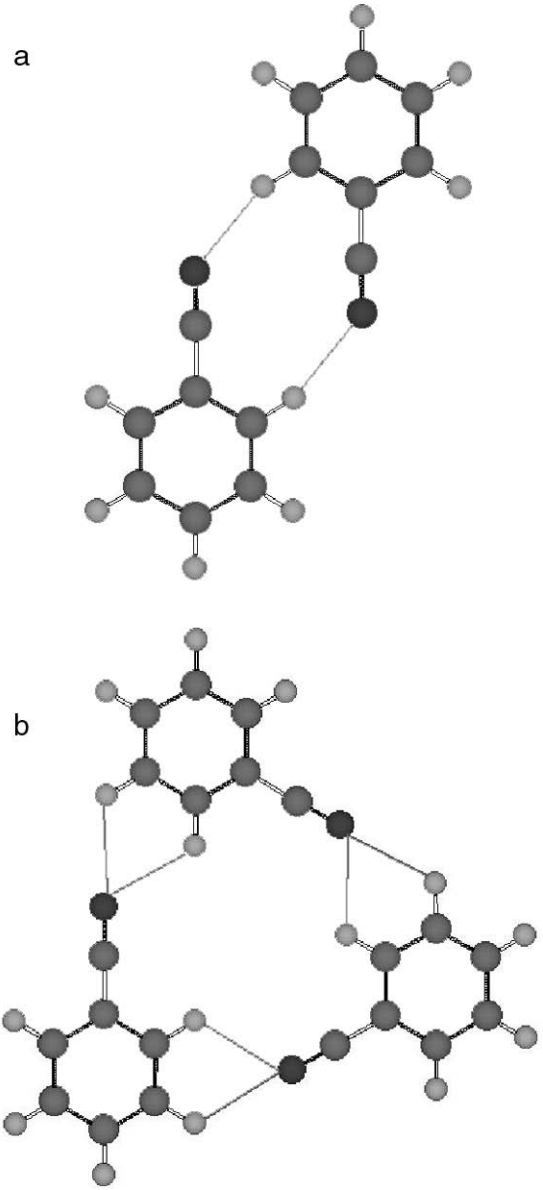

Fig. 6: Calculated molecular aggregations of (a) a cyanobenzen dimer and (b) trimer, which are obtained from ab initio molecular orbital calculations [19].

on the Au(111) surface. As shown in Fig. 8(a), identical clusters are located separately at the elbows of the herringbone patterns. From the molecular structure of CTBPP, three paired lobes are expected as a single molecule in the STM image, because a paired lobe corresponds to one di-tertiarybutyl substituent. The high-resolution STM

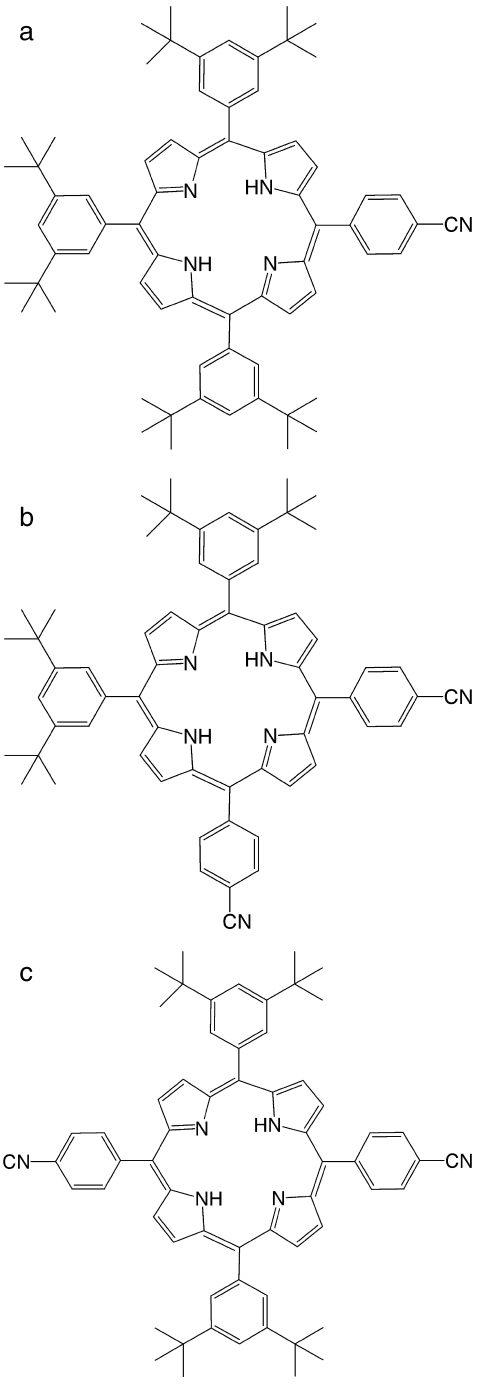

Fig. 7: Structural formula of the cyanophenyl-substituted porphyrins (a) CTBPP, (b) *cis*-BCTBPP, and (c) *trans*-BCTBPP [19].

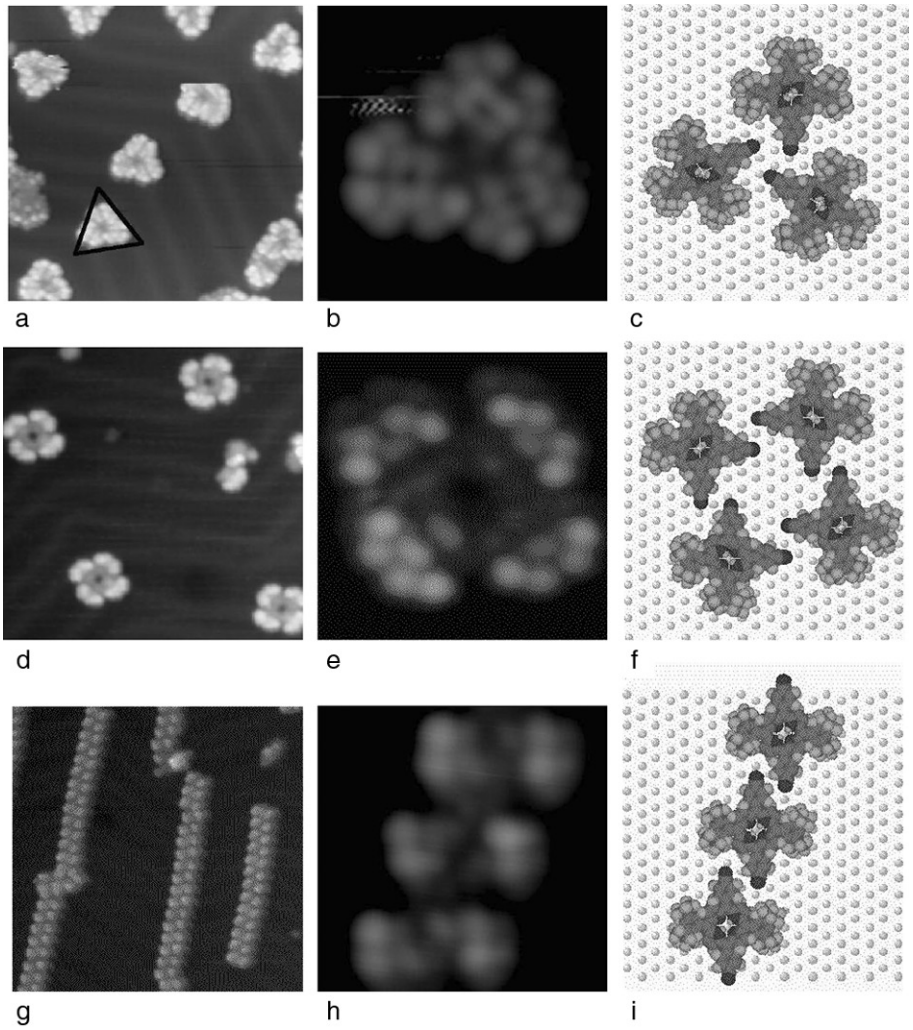

Fig. 8: STM images at 63 K of CTBPP [(a) and (b)], *cis*-BCTBPP [(d) and (e)], and *trans*-BCTBPP [(g) and (h)]. The corresponding molecular model is for (c) CTBPP, (f) *cis*-BCTBPP, and (i) *trans*-BCTBPP, respectively.

image of Fig. 8(b) shows that the triangular cluster is a CTBPP trimer. The cyanophenyl substituents are assembled into a cyclic configuration in the trimer structure of Fig. 8(c), in agreement with the cyanobenzen trimer aggregation of Fig. 7(a). Compared to the characteristic aggregation of CTBPP, we have not observed such supramolecular clusters for phenyl-tris(3,5-di-tertiarybutylphenyl) porphyrins, where the cyano substituents were removed from the CTBPP molecule. In this case, a random arrangement of the molecules was formed on the surface, confirming that the supramolecular aggregation is dominated by the cyano groups.

To probe the supramolecular aggregation in our system further, we substituted one more cyanophenyl group to give bis(4-cyanophenyl)-bis(3,5-di-tertiarybutylphenyl) porphyrin (BCTBPP), which forms two types of isomers (*cis* and *trans*) with respect to the configuration of two cyanophenyl substituents [Fig. 7(b) and (c)]. Fig. 8(d) and (e) shows that the *cis*-BCTBPP molecules are aggregated into a supramolecular tetramer. In this structure, the antiparallel intermolecular connections of all the cyanophenyl substituents lead to a macrocyclic arrangement of the porphyrin molecules, forming a molecular ring [Fig. 8(f)].

In contrast to the macrocyclic clusters of CTBPP and *cis*-BCTBPP, sequential aggregation was achieved for the *trans*-BCTBPP molecules, where two cyanophenyl groups were substituted at the *trans* positions. Fig. 8(g) shows the STM image of the Au(111) surface after deposition of the *trans*-BCTBPP molecules. In this structure, the antiparallel configuration between the cyanophenyl substituents results in a linear arrangement of the *trans*-BCTBPP molecules, forming supramolecular wires [Fig. 8(h) and (i)]. In the STM images, most of the individual wires extended across the elbows of the herringbone patterns, because the molecules were initially nucleated at the elbows. Furthermore, it is remarkable that the maximum length of the straight wire was above 100 nm, although some branches are also formed due to the three-fold symmetry of Au(111).

5. Summary

The controlled aggregation of porphyrins has succeeded on a gold surface, which was visualized by low-temperature STM. On this surface, monomer, trimer, tetramer, or wire-like arrangements were controlled by local substituent interactions, and these structures were spontaneously and selectively formed by changing substituents. We believe the selective aggregation approach should become a general strategy for the rational design and construction of desired molecular architectures on substrate surfaces.

References

1. Y. Wada, M. Tsukada, M. Fujihira, K. Matsushige, T. Ogawa, M. Haga, and S. Tanaka, Jpn. J. Appl. Phys. **39**, 3825 (2000).
2. C. Joachim, J. K. Gimzewski, and A. Aviram, Nature **408**, 541 (2000).
3. J.-M. Lehn, *Supramolecular Chemistry: Concept and Perspectives* (VCH, Weinheim, 1995).
4. H.-J. Guntherodt and R. Wisendanger (editors), *Scanning Tunneling Microscopy I* (Springer-Verlag, 1994).
5. T.A. Jung, R.R. Schlittler, J.K. Gimzewski, H. Tang, and C. Joachim, Science **271**, 181 (1996).
6. T.A. Jung, R.R. Schlittler, and J.K. Gimzewski, Nature **386**, 696 (1997).
7. G.P. Lopinski, D.J. Mofatt, D.D.M. Wayner, and R.A. Wolkow, Nature **392**, 909 (1998).
8. M.O. Lorenzo, C.J. Baddeley, C. Muryn, and R. Raval, Nature **404**, 376 (2000).
9. F. Moresco, G. Meyer, K.-H. Rieder, H. Tang, A. Gourdon, and C. Joachim, Phys. Rev. Lett. **86**, 672 (2001).
10. M. Frukawa, H. Tanaka, K. Sugiura, Y. Sakata, and T. Kawai, Surf. Sci. Lett. **445**, L58 (2000).

11. J.V. Barth, J. Weckesser, P. Gunter, L. Burgi, O. Jeandepeux, and K. Kern, Angew. Chem. Int. Ed. **39**, 1230 (2000).
12. M. Bohringer, K. Morgenstern, W.-D. Schneider, R. Berndt, F. Mauri, A.D. Vita, and R. Car, Phys. Rev. Lett. **83**, 324 (1999).
13. K. Sugiura, K. Iwasaki, K. Umishita, S. Hino, H. Ogata, S. Miyajima, and T. Sakata, Chem. Lett. 841 (1999).
14. U. Harten, A.M. Lahee, T. Peter, and Ch. Woll, Phys. Rev. Lett. **54**, 2619 (1985).
15. J.V. Barth, H. Brune, G. Etrl, and B.J. Behm, Phys. Rev. B **42**, 9307 (1990).
16. D.D. Chambliss, R.J. Wilson, and S. Chiang, Phys. Rev. Lett. **66**, 1721 (1991).
17. T. Yokoyama, S. Yokoyama, T. Kamikado, and S. Mashiko, J. Chem. Phys. **115**, 3814 (2001).
18. M.J.S. Dewar, E.G. Zoebisch, E.F. Healy, and J.J.P. Stewart, J. Am. Chem. Soc. **107**, 3092 (1985).
19. T. Yokoyama, S. Yokoyama, T. Kamikado, Y. Okuno, and S. Mashiko, Nature **413**, 619 (2001).
20. Y. Okuno, T. Yokoyama, S. Yokoyama, T. Kamikado, and S. Mashiko, J. Am. Chem. Soc. **124**, 7218 (2002).
21. M.J. Frisch, G.W. Trucks, H.B. Schlegel, G.E. Scuseria, M.A. Robb, J.R. Cheeseman, V.G. Zakrzewski, J.A. Montgomery, R.E. Stratmann, J.C. Burant, S. Dapprich, J.M. Millam, A.D. Daniels, K.N. Kudin, M.C. Strain, O. Farkas, J. Tomasi, V.A. Petersson, P.Y. Ayala, Q. Cui, K. Morokuma, D.K. Malick, A.D. Rabuck, K. Raghavachari, J.B. Foresman, J. Cioslowski, J.V. Oritiz, B.B. Stefanov, G. Liu, A. Liashenko, P. Piskorz, I. Komaromi, R. Gomperts, R.L. Martin, D.J. Fox, T. Keith, M.A. Al-Laham, C.Y. Peng, A. Nanayakkara, C. Gonzalez, M. Challacombe, P.M.W. Gill, B.G. Johnson, W. Chen, M.W. Wong, J.L. Andres, M. Heak-Godon, E.S. Replogle, and J.A. Pople, *Gaussian 98*, version A,7 (Gaussian Inc., Pittsburgh, PA, 1998).